Charles University

Faculty of Science

Study programme: Clinical and toxicological analysis

Branch of study: NKATA

Bc. Marek Straka

Determination of cesium in aqueous extracts of cement samples

Stanovení cesia ve vodných výluzích cementových vzorků

Type of thesis:

Diploma thesis

Supervisor:

RNDr. Jakub Hraníček, Ph.D.

Prague, 2022

Declaration

I declare that I carried out this diploma thesis independently, and only with the cited sources, literature and other professional sources. I declare that this thesis has not been used to gain any other academic title.

In Prague on 25.8.2022 Marek Straka

Acknowledgement

I would like to thank all my family and friends for support.

Abstract

Cement is widely used as a solidification material of low and intermediate level radioactive waste containing caesium before shallow land burial. The aim of this thesis was to extract caesium out of seventeen cement samples with six different cement binder compositions, by extraction with deionized water, then determine the amount of caesium in the extracts and look for trends in the extract Cs concentrations with various extraction duration. Cement samples, with stable caesium nuclide, were used to simulate retention of caesium in immobilized radioactive waste. Ten extractions from each sample in total were made with time ranging from 2 to 1032 hours. Atomic absorption spectrometry with flame atomization, using acetylene as fuel and air as oxidant, was used for caesium determination. This method was optimized and the addition of KCl serving as ionization buffer for better results was explored and compared.

Keywords

Atomic absorption spectrometry, flame atomization, caesium, extraction,

Abstrakt

Cement je nejčastěji využívaný jako materiál pro ztužení nízko a středně radioaktivního odpadu obsahujícího cesium, před mělkým uskladněním v zemi. Cílem práce bylo extrahovat cesium ze sedmnácti cementových vzorků s šesti různými složeními cementové směsi pomocí deionizované vody, následně stanovit množství cesia v extraktech a sledovat trendy ve změnách koncentrace cesia při různých délkách extrakce. Cementové vzorky obsahující stabilní nuklidy cesia byly použity k simulaci retence cesia v imobilizovaném radioaktivním odpadu. Celkem bylo provedeno deset extrakcí z každého vzorku, s rozsahem délky extrakce od 2 do 1032 hodin. Pro stanovení cesia byla použita metoda atomové absorpční spektrometrie s plamenovou atomizací využívající acetylen jako palivo a vzduch jako oxidant. Tato metoda byla optimalizována, a zároveň byla prozkoumána a komparována možnost přidání ionizačního pufru ve formě KCl pro lepší výsledky.

Klíčová slova

Atomová absorpční spektrometrie, plamenová atomizace, cesium, extrakce

Contents

List of abbreviations

AAS – atomic absorption spectrometry

ASD – absolute standard deviation

Al - aluminium

Al_2O_3 – aluminium oxide

Ca - calcium

CaO – calcium oxide

Cs - caesium

CSAC – calcium suplfoaluminate cement

CSH - calcium hydrate gel-like phase

CTU – Czech Technical University in Prague

F-AAS – atomic absorption spectrometry with flame atomization

Fe_2O_3 – ferric oxide

HCL – hollow cathode lamp

ICP-MS – inductively coupled plasma mass spectrometry

LOD – limit of detection

LOQ – limit of quantification

MS – mass spectrometry

SiO_2 – silicon dioxide

Sr – strontium

wt% - percentage by weight

w/c – water to cement ratio

1. Goals and objectives

- Optimize method of determination by atomic absorption spectrometry
- Extract caesium from cement block samples
- Identify trends in caesium concentration values in extracts
- Compare results with and without addition of ionization buffer

2. Introduction

2.1. Alkali Metals

Alkali metals are a group of extremely reactive elements that belong to the first group of periodic table with ns^1 electron configuration, which explains their chemical and physical properties. In pure form they are very soft, have a characteristic silver metallic colour and a relatively low melting point. Due to their high reactivity they have to be preserved in an inert atmosphere, or submerged in kerosene. Alkali metals include lithium, sodium, potassium, rubidium and caesium. Sodium and potassium are abundant in the earth`s crust but since they are present mainly in the form of compounds their recovery is an energy intensive process. [2,3,4]

2.1.1. Caesium

Caesium with the lowest melting point among alkali metals is also the rarest, and only in recent history it began to be used commercially. It was discovered in 1860 in mineral water, by a newly developed method of flame spectrometry. In nature it is present as a monoisotope, and it can be found near the lake Bernic in Canada, in the form of a zeolite mineral, pollucite.[5] The main source of caesium is, as a by-product of lithium processing. Commercial use for Cs is in photocells, as it easily releases electrons under the influence of light.[5] It is also used in science in atomic clocks, where they use its transfer between basic and specific excited state and monitor the frequency of emitted electromagnetic radiation.[2,3] Cs is a toxic pollutant and is not biodegradable, which makes monitoring of the Cs content in the environment very important.[6] After the Chernobyl accident in 1986, radioactive caesium ^{137}Cs has hugely settled in in forests of Sweden. These radionuclides of Cs can be leached into the soil during rainfall, and are absorbed by wild fungi and game, often eaten by Swedish population, which is one of many cases for monitoring content of Cs in the environment.[7,8]

2.1.2. Caesium determination

The easiest proof of presence, is to let Cs react with hydrochloric acid and heat it on a Bunsen burner. It gives a specific blue colour flame. For quantitative analysis, the most common method is atomic absorption spectrometry, which also utilizes its characteristic atomic

spectrum.[2,3] However, methods such as gamma-ray spectrometric determination, resonance ionization spectroscopy coupled with time-of-flight mass-selective ion detection, and a semiconductor diode laser spectrometer in a graphite-tube furnace can also be used for determination.[9,10,11] Gravimetric determination by precipitation by tetraphenylborate and radiochemical or epithermal neutron activation can also be used to determine caesium.[12] AAS measurements can be done either with flame, or electrothermal atomization.[13] Electrothermal atomization is relatively repeatable and reasonably efficient.[14]

Inductively coupled plasma mass spectrometry (ICP-MS) and flame atomic absorption spectrometry are frequently used methods for Cs determination. Both ICP-MS and F-AAS systems were available at our faculty. But due to the high amount of matrix present in the extracts, low sensitivity to interferences, robustness, less time-consuming sample preparation, lower operation cost and sufficient sensitivity, F-AAS was used for Cs determination.[13,15]

2.2. Atomic absorption spectrometry

Atomic absorption spectrometry (AAS) is a highly selective analytical method and one of the most simple, economical, and widely used techniques for element analysis.

Figure. 2.1. A photograph of GBC 933 AA atomic absorption spectrometer.

2.2.1. History

History of spectroscopy goes far into the 17th century when the first experiments with solar spectrum were performed. At the beginning of 19th century, the determination of exact position of spectrum lines was established. The explanation of origin of spectral lines came in 1859-1860 which opened the door for absorption and emission spectroscopy to be used for measurements in astronomy and chemistry.[16]

The first atomic absorption spectrometer was made in 1959 and was gradually developed to its current state. But its actual worldwide popularity was not immediate, due to the problems with low sensitivity caused by very narrow absorption lines. This problem was solved by using a special radiation source that radiates only a desired wavelength.[16]

2.2.2. Principle of atomic absorption spectrometry

It is based on the absorption of radiation, emitted by primary radiation source, by free atoms of the element which are usually in ground state. The determination is based on the Lambert-Beer law for absorption by free atoms of an element in gaseous state. The amount of radiation

absorbed is relative to the concentration of the element and is the main principle for quantitative determination. Spectral range used with AAS is 190-900 nm and the selected wavelength for the analysis itself corresponds to the transition of the atoms between ground state and excited level. For the analysis itself only resonation transitions (transitions between ground state and excited state) are used. [1,17,18]

2.2.3. Instrumentation of AAS

Typical atomic absorption spectrometer consists of primary radiation source, source of free atoms with sample introduction system, optical dispersive system, detector and electronics for data acquisition and processing.

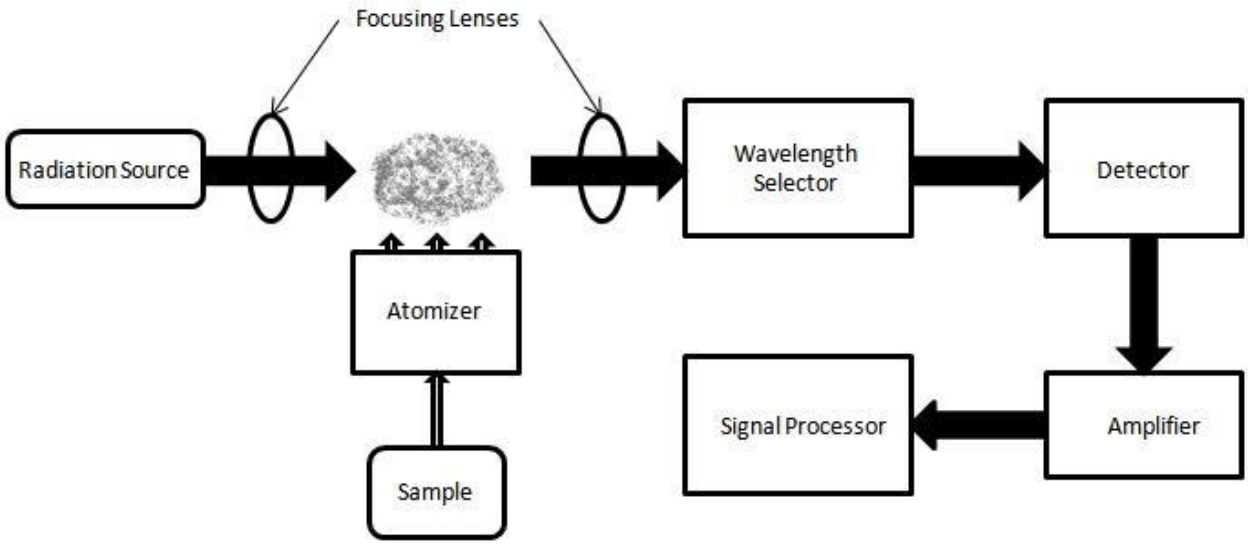

Figure 2.2. Diagram of atomic absorption spectrograph [19]

2.2.3. Primary radiation source

The typical primary radiation source is usually a hollow cathode lamp (HCL) or electrodeless discharge lamp.[1] HCL consists of two electrodes encased in a glass tube filled with Ar or Ne gas at low pressure of about 100-200 Pa.[17] At the end of the tube is a silica window transparent to UV-vis spectral range for light transmission. Voltage at the range of 200-600 V is applied on electrodes which leads to a current of 3-25 mA. Positive ions generated by the discharge are accelerated and crash into cathode releasing free atoms of the metal. The released atoms are excited by crashing into the positive gas ions or free

electrons. Excited atoms returning to ground state radiate radiation specific to the used cathode material. For anode a heat resistant metal like zirconium, titanium, tantalum, tungsten or nickel is used to prolong its lifetime.[1,17] The cathode is made out of highly pure metal or a mix of metals shaped into a hollow cylinder and shielded by a glass shield to cover the rest of the lamp from sputtered atoms of the metal, which happens during electrical discharge.[1]

The main disadvantage of HCL is that it is element specific and can only measure the element which the cathode is made out of. This makes a multi-element analysis expensive and slow.[20] In the case of cathode being made out of several elements, more elements can be measured with one lamp, but at the cost of its lifetime since different elements have various volatilities.[1]

To eliminate the need to change the radiation source for every new element to be determined a continuum source is used. Problem with using continuum source is that only a small fraction of light is of the characteristic wavelength of the element. This would result in a low analytical sensitivity. To bypass this issue an Echelle grating monochromators with smaller spectral bandpass are used. It used to be the case, that the continuum radiation sources were not capable of reaching as high sensitivity as radiation sources with narrower linewidth.[1] However, recent development in AAS technology has changed that.[21] The most used continuum radiation sources are deuterium lamp and high intensity xenon arc lamp, which is preferred for its higher brilliance.[1]

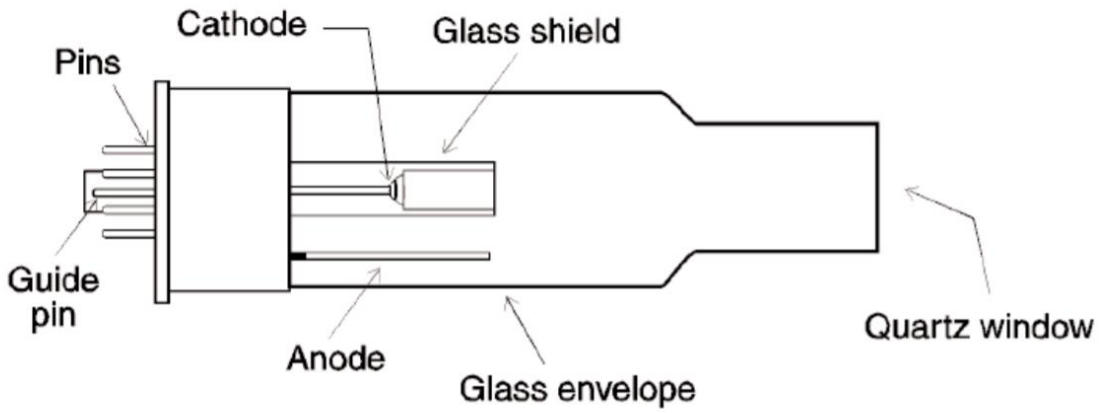

Figure 2.3. Diagram of a typical hollow cathode lamp.[22]

2.2.4. Atomization

For the absorption of radiation by free atoms of the sample to be observed, the atoms of the sample need to be in an atomic and gaseous state.[1] The role of the atomizer is to efficiently convert the sample into free atoms mostly in ground state. Free atoms must be located in the light path between the radiation source and dispersive system.[18] The most common methods for production of free atoms in gaseous state use thermal energy. For example flame atomization burns fuel and oxidizer, electrothermal atomization uses graphite tubes for sample introduction with electrical heating, and quartz tube atomizers use either electrical or flame heating. The efficiency of this transfer directly correlates to the sensitivity of the method.[1]

Flame atomization uses acetylene as fuel and air or nitrous oxide as an oxidizer. Due to the high temperature of the flame, the sample is evaporated and thermal decomposition of the sample compounds to monoxides and eventually to free atoms occurs. To ensure ideal mixture flow rate different sized slit of titanium burner is used for different oxidizer and fuel mixtures, so the mixture flow speed is higher than the burning speed.[17]

2.2.5. Monochromator

The role of monochromator is to isolate different wavelengths so that only radiation of required wavelength will pass to the detector. Monochromators are usually equipped with a diffraction grating that separates these wavelengths. By rotating the grating, you can achieve passing of radiation of different wavelengths through the exit slit. Range of wavelengths that can pass through the monochromator is called spectral bandwidth, and is limited by exit slit width and dispersion of monochromator.[23] Placement of a monochromator between flame and photo-multiplier excludes most of the radiation created by chemiluminescent reactions in the flame.[24]

2.2.6. Detector

Most of the atomic absorption spectrometers are equipped for measuring in UV-VIS spectral range. The detector uses photomultiplier, to turn radiation into signal, and is located after the exit slit. The detector then sends the signal into the computer, where changes in signal intensity are registered.[23]

2.3. Cement

Cement is a binder material used in nuclear waste disposal as a construction material of nuclear waste facilities. It also serves as a structural element for storing the low-level and intermediate-level radioactive waste itself, its immobilization and shielding. The ability to bind to a wide variety of materials, such as metals and minerals, to shield metals used for structural reinforcement from corrosion, low cost and high durability in natural environment makes it an ideal material for nuclear waste disposal. [25,26]

2.3.1. Cement mixtures

Cement can be classified into two basic categories: hydraulic and non-hydraulic cements. Hydraulic cement will harden even when placed underwater. Non-hydraulic cement will only disperse in the water, and will not harden and bind to other materials, e.g., gypsum-based cements. Gypsum can be added to the cement mixture as a retarder to delay hardening of the cement mixture. The prolongation of setting time can be crucial in some circumstances e.g., transportation, concrete mixing and placement. [25,26]

Portland cement is classified as hydraulic cement, and is the most used among cement matrices in construction and also in nuclear waste disposal, considering its suitable properties, and problems connected with production of specific cement matrices in smaller quantities. Only five types of Portland cement are in wide commercial production, with modern day cement kilns rarely producing less than 500 to 800 tons per day.[25,26] However, some nuclear operations use different types of cement, admixtures and supplementary cementing materials. Portland cement has four main components. It is based on Calcium oxide with 62-68% content of CaO by weight, followed by SiO_2 with 21-24%, Al_2O_3 with 4-8% and Fe_2O_3 with 1-6% of content by weight. It`s exact chemical composition is not specified and often depends on its national or regional requirements and intended use. What makes it more complicated is that often cement specifications can be either prescriptive or performance based. Performance based properties are certainly important, but are not sufficient for nuclear waste storage use. Whilst the exact chemical and performance-based properties of cement can be known. The frequent use of additives, and considering the high contribution of these additives to immobilization potential, complicates prediction models even further.[25,26]

When Portland cement comes to contact with sulphate containing brines its Ca and Al components react and expand, causing cracking. This problem can be solved by using calcium sulfoaluminate cement (CSAC). CSAC is also classified as hydraulic cement, has been commercially made in China since 1975, and can be an alternative to Portland cement. It has lower Al_2O_3 content compared to Portland cement, which improves its sulphate resistance. CSAC sets rapidly, compared to Portland cement, and requires a retarder to provide sufficient period of workability. CSAC gains strength more rapidly, shrinks slightly more compared to Portland cement, but during hardening upon hydration releases heat more rapidly and has to be carefully managed. [25,26]

Water to cement ratio (*w/c*) is one of parameters that needs to be specified for better reproducibility of results. Increase in *w/c* ratio increases fluidity of the mix, and also allows for a higher proportion of liquid waste to be incorporated into the mix. Theoretical *w/c* ratio for Portland cement is 0.25. Such low *w/c* ratio however would cause the cement mix to be stiff, poorly workable and would be ineffective for radioactive waste disposal. Excessive water in the mix is incorporated into the cement matrix and conserved in pores, known as pore water. Large surplus of water increases the permeability of hardened cement. If the intended use of the cement is to act as a physical barrier for water, the *w/c* ratio needs to be carefully considered and taken into account.[26]

2.3.2. Cement additives

Addition of cement modifiers, such as silica, slag and fly ash, metakaolin and zeolite can modify the cement properties. E.g., reduce viscosity, increase strength at long ages, decrease permeability and pore volume, or change chemical properties of the cement mix. These modifications can play an important role in nuclear waste disposal use. Effect of addition of metakaolin to the concrete mix has been reported to reduce permeability, while increasing total pore volume. This was due to higher content of small volume pores, with diameter less than 20 μm. Amount of CSH gel also slightly increased with addition of metakaolin, which could contribute to higher immobilization capacity.[27] Addition of zeolites has also been reported to decrease leaching rate of $_{137}Cs$ and $_{90}Sr$ from cement matrices, due to their small particle size and large surface area. These properties helped reduce pore size and reduce permeability. Use of zeolites in removal of radioisotopes from aqueous nuclear waste, their

good compatibility with cement mixes, selectivity, and need to dispose of used zeolites in solid cement matrices, makes them a suitable additive.[28]

2.3.3. Immobilization mechanisms

Immobilization potential of cement is either chemical or physical, with chemical potential considered to be more important for long-term storage.[26] High internal pH of pore water in cement, large surface area with high sorption capacity, low redox potential in slag systems and functioning as a physical barrier are the main contributors to its immobilization potential. Retention of pH in pore water above certain level being one of essential parameters for repository lifetime. Cementitious materials also influence chemical properties of the surrounding repository, providing alkaline conditions. These increase immobilization by raising sorption and lowering solubility.[25,29]

Main physical mechanism is surface sorption of the binding phase in Portland cement which is a calcium hydrate gel-like phase (CSH). With high specific surface around 50-200 $m^2 \cdot g^{-1}$, and a known tendency to absorb both cations and anions like Cs and sulphate, makes it a primary source of sorption for Cs.[25,30] Considering these conditions, transport of radionuclides is primarily by diffusion processes reduced by sorption mechanisms.

Diffusion of ions in cement-based materials mostly depends on pore structure. Porosity, pore size, pore distribution and their interconnectivity are considered to be the major aspects that affect diffusion of ions. Diffusion of Cs though cement is considered as “double porosity” with different diffusion paths on the surface and on the inner part of the sample.[29] Pore sizes in cement materials range from 10 μm to 0.5 nm.[31] Larger pores ranging from 10 μm to 10 nm are unfilled cavities between cement grains. Smaller pores ranging from 10 nm to 0.5 nm are part of the internal porosity of CSH gel. The diffusion takes place primarily through larger pores with a width of a few microns, and gradually moves into the interior of the cement, to the intact submicron pores.[32]

3. Experimental section

3.1. Reagents

Extraction of Cs was carried out in 1000mL polypropylene plastic reagent wide neck bottles. Deionized water (< 0.07 μS ULTRAPUR) was used for extraction. Ionization buffer was prepared from 100 $g \cdot L^{-1}$ KCl solution (prepared from 99.5-100.5 % KCl, Sigma-Aldrich, Germany) by dilution in deionized water. Cs standards (prepared from Cesium Standard for AAS, 1000 $mg \cdot L^{-1} \pm 4$ $mg \cdot L^{-1}$ Sigma-Aldrich, Germany) were prepared by dilution in deionized water.

3.2. Instrumentation

Cs determination was done on a GBC 933 AA (GBC Scientific Equipment Australia) atomic absorption spectrometer with flame atomization (acetylene-air). A Varian Techtron PTY hollow cathode lamp was used as a light source. Input parameters are listed in the table 3.1. Compressed acetylene was produced by Linde, Czech Republic and air was supplied by BAMAX Silent OLE compressor.

Table 3.1. Input parameters for GBC 933 AA.

Element	Cs
Wavelength [nm]	852.1
Supply current [mA]	15
Number of repetitions	3
Acetylene flow rate [$mL \cdot s^{-1}$]	24
Air flow rate [$mL \cdot s^{-1}$]	72

3.3. Samples

Cement is widely used as a solidification material of low and intermediate level radioactive waste containing Cs before shallow land burial.[33] Material for this use must have a suitable mechanical properties, permeability and high sorption capacity for radionuclides, which ensure its low leachability.[34,35] However, the retention of Cs in cement matrix is negligible due to its

rather high water mobility and low chemical interaction with the cement.[36] The sorption of Cs is low, and diffusivity of Cs is high in hydrated cement. A mix of cement with a material, with significant sorption capacity is a common practice in storage of radioactive waste.

Cement samples, that were used, simulate immobilized radioactive waste. Normally the Cs found in the cement are radioactive nuclides, and extractability of Cs is determined by change of radioactivity over time. But in this case a stable nuclide was present in the sample and extractability was determined using AAS.[37,38]

The cement samples used, acquired from CTU, were made from a model evaporate concentrate without radionuclides based on a study by Szalo and Žatkulák.[39] It composed of sodium hydroxide (72.9 $g \cdot L^{-1}$), potassium hydroxide (14.9 $g \cdot L^{-1}$), boric acid (76.0 $g \cdot L^{-1}$), sodium sulfate (3.5 $g \cdot L^{-1}$), sodium nitrite (14.5 $g \cdot L^{-1}$), sodium nitrate (27.1 $g \cdot L^{-1}$), sodium chloride (2.0 $g \cdot L^{-1}$), citric acid (1.6 $g \cdot L^{-1}$) and oxalic acid dihydrate (2.8 $g \cdot L^{-1}$). These separate compounds were mixed with distilled water that was used as a mixing water with cement composites.

The six different cement composite mixes were used as binders, based on previous studies and experiments (see table 3.2.)[40,41,42,43,44]. Water-binder ratio of 0.4 and 0.5 was used.

Table 3.2. Cement binder composition.

Abbreviation	Composition
SAC	100 % calcium-sulpho-aluminate cement
NP	50 % non-gypsum cement + 50 % Portland cement 42.5 R
NM	50 % non-gypsum cement + 50 % metakaolin
NP_M	50 % non-gypsum cement + 45 % Portland cement 42.5 R + 5 % metakaolin
NP_Z	50 % non-gypsum cement + 45 % Portland cement 42.5 R + 5 % natural zeolite
NM_Z	50 % non-gypsum cement + 45 % metakaolin + 5 % natural zeolite

To avoid volume changes a 40 wt% of pure fine silica aggregate, supplied by Sklopísek Střeleč, Czech Republic, was added.

In total seventeen samples were obtained. The cement samples were of square prism shape with 2x2x10 cm dimensions. All samples were submerged in deionized water for thirty seconds

and placed in a polypropylene plastic 1000mL bottle, with 880 mL of deionized water. After two hours, cement block was removed with plastic tweezers, left to drip and placed in another bottle for another extraction. This process took less than five seconds each time. The solution was stirred and two 50mL samples were taken from each bottle into 50mL centrifuge test tubes. The remaining content was disposed of, and the bottle was rinsed with deionized water. A control measurement was done for impurities in the bottle. This procedure was repeated ten times in total for each extract, with extraction time ranging from 2 to 1032 hours and was done according to the American National Standard ANSI/ANS-16.1-2003. For each sample a new fresh deionized water was used, that was controlled for Cs impurities before sample insertion. Duration of extractions is listed in table 3.3. When cement sample comes in contact with deionized water, the soluble compounds in the sample move into the surrounding water. This is caused by the dissolution, or chemical reaction, with chemical compounds in the deionized water.[45]

Table 3.3. List of duration of extractions.

Number	Duration [h]
1	2
2	5
3	17
4	24
5	24
6	24
7	24
8	336
9	672
10	1032

4. Optimization of method and measurement conditions

To achieve accurate and repeatable results a method optimalization was performed. Measurement method was optimized for beam height and acetylene flow rate. LOD and LOQ were determined.

4.1. Optimization of AAS

Beam height and acetylene flow rate were optimized for AAS spectrometer. Actual acetylene flow rate had to be experimentally measured, since the AAS spectrometer adjustment knob for acetylene flow rate, air flow rate and beam height is using relative units. This was done using acetylene intake hose introduced inside a reversed graduated cylinder submerged in water, filled with water and measuring the volume of expelled water per time. Values of acetylene flow rate obtained with this method are thus only indicative. Air flow rate could not be measured using this method since for the air to have restricted flow rate it needs resistance in the fog chamber. Air flow rate was calculated from data measured for acetylene flow rate, based on the presumption of AAS spectrometer using the same relative units for acetylene and air flow rate. Beam height was measured using a square ruler.

Five different acetylene flow rates were tested and we can see a steady decline of Cs signal with increasing acetylene flow rate (Figure 4.1.A). This is due to dilution of free Cs atoms in the optical path with higher volume of acetylene introduced. Optimal flow rate for acetylene was determined to be 24 $mL \cdot s^{-1}$.

The optimization of beam height was done for beam heights between 4 and 23 mm. In figure 4.1.B we can see gradual increase in absorbance with decreasing beam height. This is due to the optical path being closer to the space where atomization occurs and lower free Cs atoms dissipation. Optimal beam height was determined to be 4 mm.
The list of all optimized and calculated parameters is listed in table 4.1.

A)

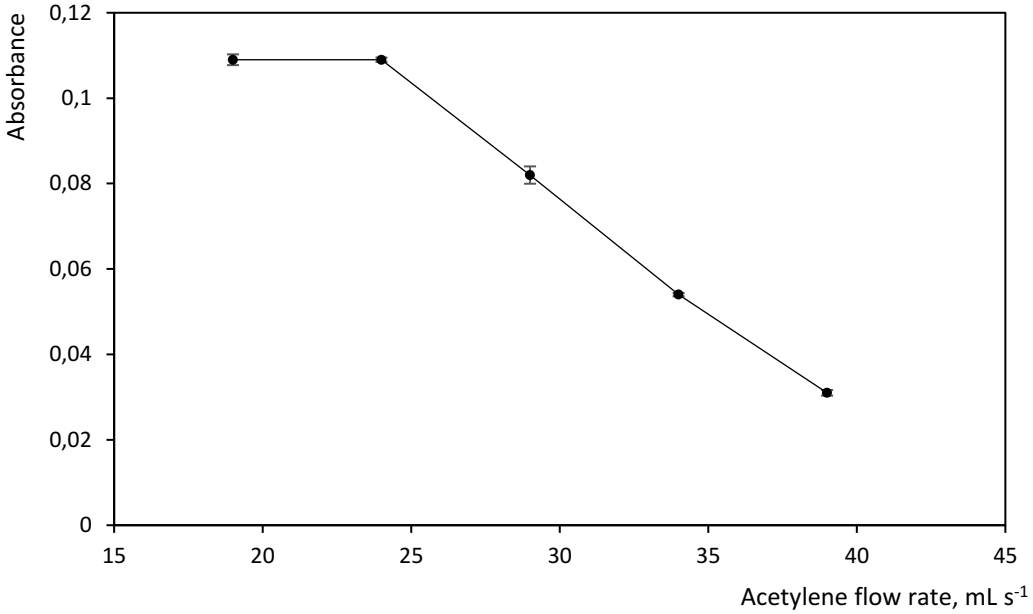

B)

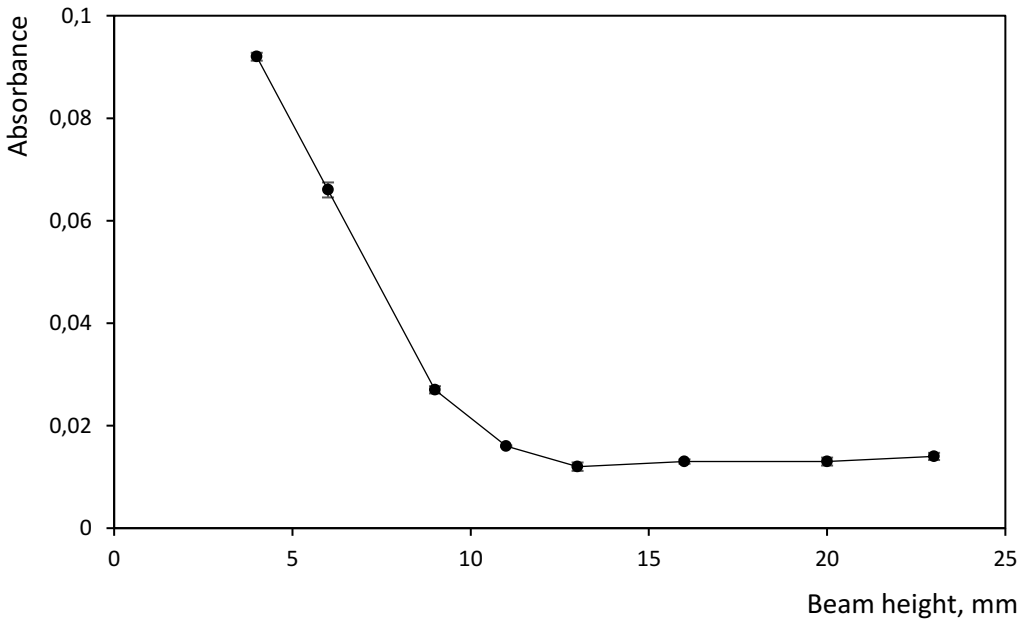

Figure 4.1. Effect of different acetylene flow rate (A) and beam height (B) on Cs signal intensity with F-AAS detection. Cs standard concentration 10 $mg \cdot L^{-1}$. If not being a parameter to be optimized, beam height was 4 mm, air flow rate 72 $mL \cdot s^{-1}$ and acetylene

flow rate at 24 $mL \cdot s^{-1}$. HCl was operated at a lamp current of 15.0 mA and a wavelength of 852.1 nm.

Table 4.1. Summary of optimal conditions and calculated limits of detection and quantification

Measured parameter	Optimal/calculated value
Beam height	4 mm
Acetylene flow rate	24 $mL \cdot s^{-1}$
Air flow rate	72 $mL \cdot s^{-1}$
LOD	0.116 $mg \cdot L^{-1}$
LOQ	0.386 $mg \cdot L^{-1}$

4.2. Limit of detection

Five measurements were made with Cs concentration of 10 $mg \cdot L^{-1}$, each with 3 repetitions. LOD was calculated to be 0.116 $mg \cdot L^{-1}$ and LOQ 0.386 $mg \cdot L^{-1}$ (table 4.2.) as depicted below, character b being regression line slope.

Table 4.2. Results of standards measurements with calculated standard deviation, regression line slope, limit of detection and limit of quantification.

Sample number	Concentration of Cs
1	9.89 $mg \cdot L^{-1}$
2	9.79 $mg \cdot L^{-1}$
3	9.48 $mg \cdot L^{-1}$
4	9.97 $mg \cdot L^{-1}$
5	9.20 $mg \cdot L^{-1}$
Average	9.47 $mg \cdot L^{-1}$
Standard deviation (SD)	0.39
Regression line directive (b)	10.13
Limit of detection (LOD)	0.116 $mg \cdot L^{-1}$
Limit of quantification (LOQ)	0.386 $mg \cdot L^{-1}$

$$LOD = \frac{3 * SD}{b}$$

$$LOD = \frac{3 * 0.39}{10.13}$$

$$LOD = 0.116\ mg/L$$

$$LOQ = \frac{10 * SD}{b}$$

$$LOQ = 0.386\ \text{mg}\cdot\text{L}^{-1}$$

5. Results and discussion

In total seventeen samples of cement blocks were used. Each sample was extracted ten times. Extracts were then measured using atomic absorption spectrometry with flame atomization (F-AAS). Addition of ionization buffer was tried and tested. The possibility of influence of water source was also investigated.

5.1. Addition of ionization buffer

Ionization can be the cause of non-linearity of calibration curve. This could generate the need for larger number of calibration solutions needed, or loss of sensitivity in the lower range of concentrations, or diversion from calibration curve in higher ranges of concentrations.[46,47] The possibility of addition of ionization buffer was examined. Adding an excess of easily ionized element, such as Cs (ionization energy 3.9 eV) or K (ionization energy 4.34 eV),[48] acts as an ionization buffer by producing large excess of electrons in the flame.[46] This causes that the ionization buffer will be ionized instead of analyte, preventing a decrease in signal.[49] Both CsCl and KCl were considered to be used as ionization suppressor but due to our analyte being Cs, KCl was chosen for its better suitability, availability and lower cost as the better option.[50]

The possibility was experimentally tested with Cs standards with concentration of Cs ranging from 1 to 10 $mg \cdot L^{-1}$. Addition of ionization buffer was determined to have positive effect on absorbance level (see Figure 5.1.). The increase in absorbance level can be attributed to the partial pressure of electrons produced by ionization buffer, which shifts ionization equilibrium of the analyte in favour of uncharged atoms. Thus, if the sample contains an element other than the analyte, that is easily ionized, it decreases the ionization of the analyte while increasing its signal.[46]

However, addition of ionization buffer had no effect on trend line of extracts measurements (see Figure 5.1.), and was therefore not used for extracts.

The addition of KCl also had positive effect on linearity and accuracy. Still, the linearity of calibration curve without ionization buffer was acceptable, the determination coefficient was almost the same (0,9938 compared to 0,9978 with KCL).

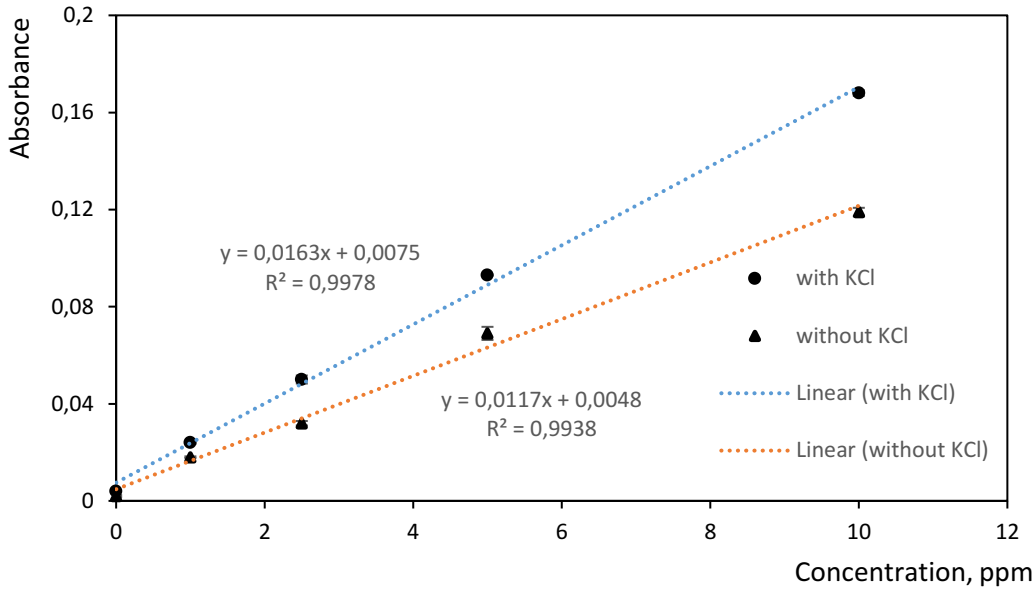

Figure 5.1. Effect of addition of KCl (ionization buffer) on Cs signal level. Cs standard concentration 10 mg·L^{-1}. Beam height was set to 4 mm, air flow rate 72 mL·s^{-1}, acetylene flow rate at 24 mL·s^{-1}. HCl was operated at a lamp current of 15.0 mA and a wavelength of 852.1 nm.

5.2. Influence of water source

To be sure that there is no influence from source of water used for Cs extraction on the results of Cs concentration in extracts, three different sources of water were tested. There was no observable effect on signal intensity and no detectable amount of Cs impurities found (table 5.1.). Since there was no effect of water source on Cs detection accuracy, ULTRAPUR deionized water source was used, as it was most available for use.

Table 5.1. Effect of water source on Cs concentration in water.

* Conductivity according to the manufacturer

[x] Values below LOD

Sample	Conductivity (µS)*	Concentration of Cs ($mg \cdot L^{-1}$)	Standard deviation
ULTRAPUR deionized water	0.07	0	0
Milli Q twice deionized water	0.055	0.001[x]	0
ROWAPUR distilled water	18.33	0.002[x]	0.0003

5.3. Results of measurement of extracts

Ten extracts in total were made out of each cement block sample and Cs concentration was measured in these extracts using F-AAS.

Extracts were separated into 6 groups based on their binder composition (table 3.2.). The measurements with addition of ionization buffer were also separated into six groups based on their binder composition.

5.3.1. Results of extracts without ionization buffer

In figure 5.2. are depicted the results of group NP which cement binder composed of 50 % non-gypsum cement and 50 % Portland cement 42.5 R. In each consecutive extraction we can see about half the concentration of Cs per hour of extraction on average. Each consecutive extraction had either a decline in Cs concentration per hour, or it stayed the same. One exception being extraction number 7 in sample NP-0,5 4 where we saw a rise in c/h from 0.16 to 0.19 $mg \cdot L^{-1}.h^{-1}$.

This phenomenon was observed with multiple other samples also, at extractions order numbers 5, 6 or 7, where we saw no, or much lower decline in c/h. E.g., figure 5.5.

sample NM-0,5 3 extraction order number 5 and 6. The water reaching intact smaller and deeper pores of the cement sample with different diffusion paths could be the explanation. This was mentioned in chapter 2.3.3., and described as “Double porosity” properties of cement.

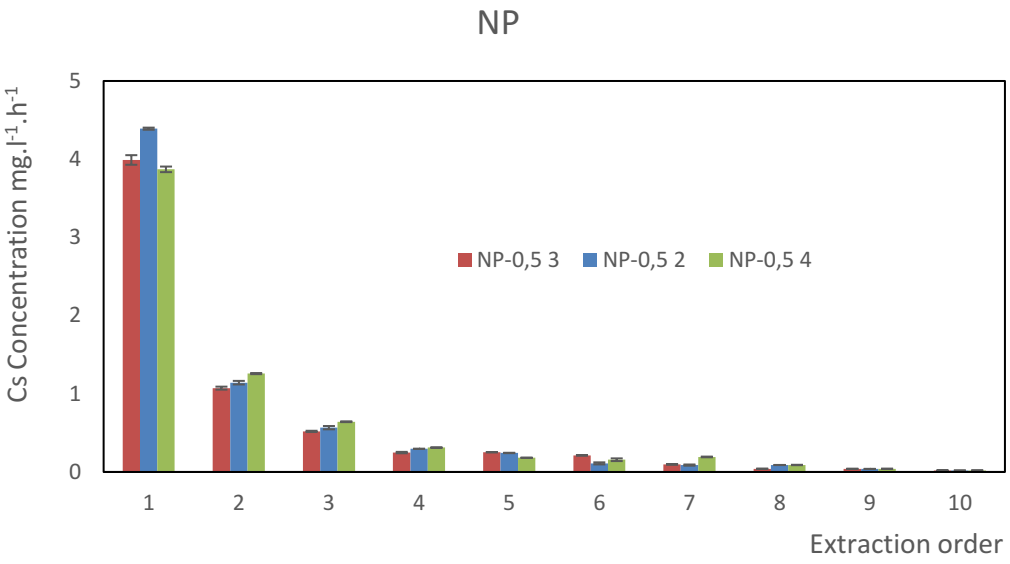

Figure 5.2. Concentration of Cs in group NP, divided by the number of hours of extraction length. Beam height was set to 4 mm, air flow rate 72 mL·s^{-1}, acetylene flow rate at 24 mL·s^{-1}. HCl was operated at a lamp current of 15.0 mA and a wavelength of 852.1 nm. Table of results is attached in appendix A in table 1, 2 and 3.

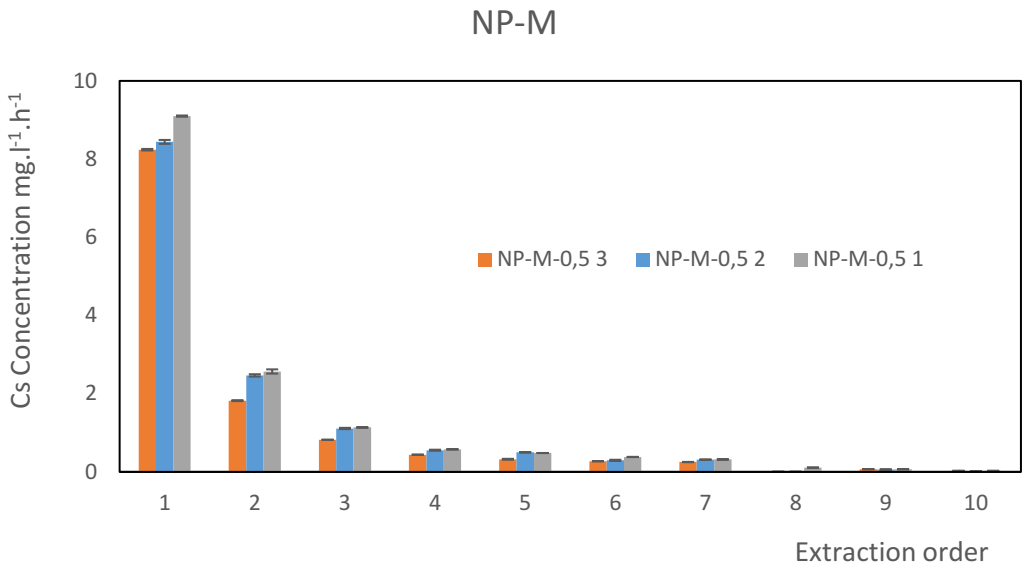

Figure 5.3. Concentration of Cs in group NP-M, divided by the number of hours of extraction length. Beam height was set to 4 mm, air flow rate 72 mL·s^{-1}, acetylene flow rate at 24 mL·s^{-1}. HCl was operated at a lamp current of 15.0 mA and a wavelength of 852.1 nm. Table of results is attached in appendix A in table 10, 11 and 12.

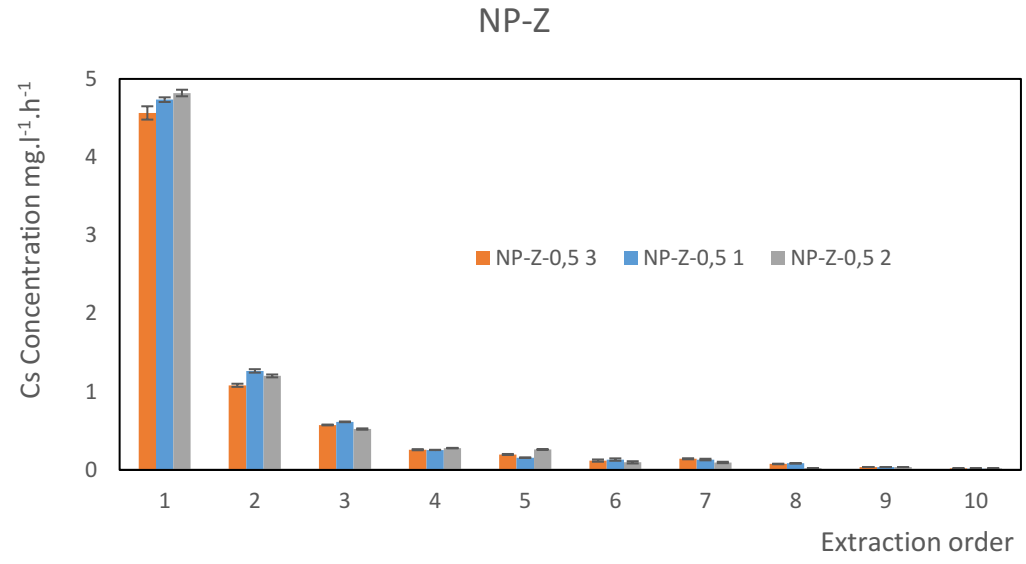

Figure 5.4. Concentration of Cs in group NP-Z, divided by the number of hours of extraction length. Beam height was set to 4 mm, air flow rate 72 mL·s^{-1}, acetylene flow rate at 24 mL·s^{-1}.

HCl was operated at a lamp current of 15.0 mA and a wavelength of 852.1 nm. Table of results is attached in appendix A in table 13, 14 and 15.

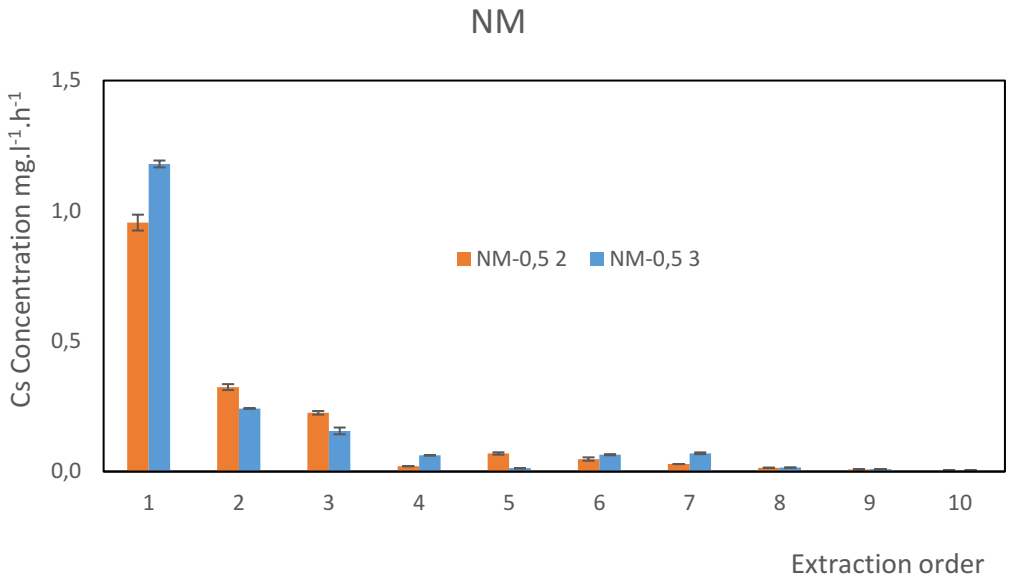

Figure 5.5. Concentration of Cs in group NM, divided by the number of hours of extraction length. Beam height was set to 4 mm, air flow rate 72 mL·s^{-1}, acetylene flow rate at 24 mL·s^{-1}. HCl was operated at a lamp current of 15.0 mA and a wavelength of 852.1 nm. Table of results is attached in appendix A in table 16 and 17.

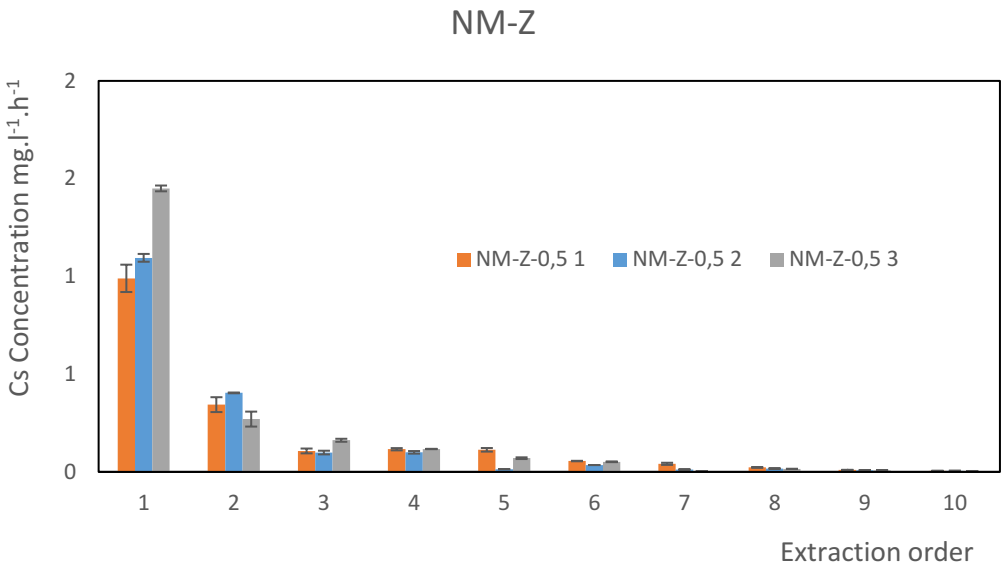

Figure 5.6. Concentration of Cs in group NM-Z, divided by the number of hours of extraction length. Beam height was set to 4 mm, air flow rate 72 mL·s^{-1}, acetylene flow rate at 24 mL·s^{-1}. HCl was operated at a lamp current of 15.0 mA and a wavelength of 852.1 nm. Table of results is attached in appendix A in table 7, 8 and 9.

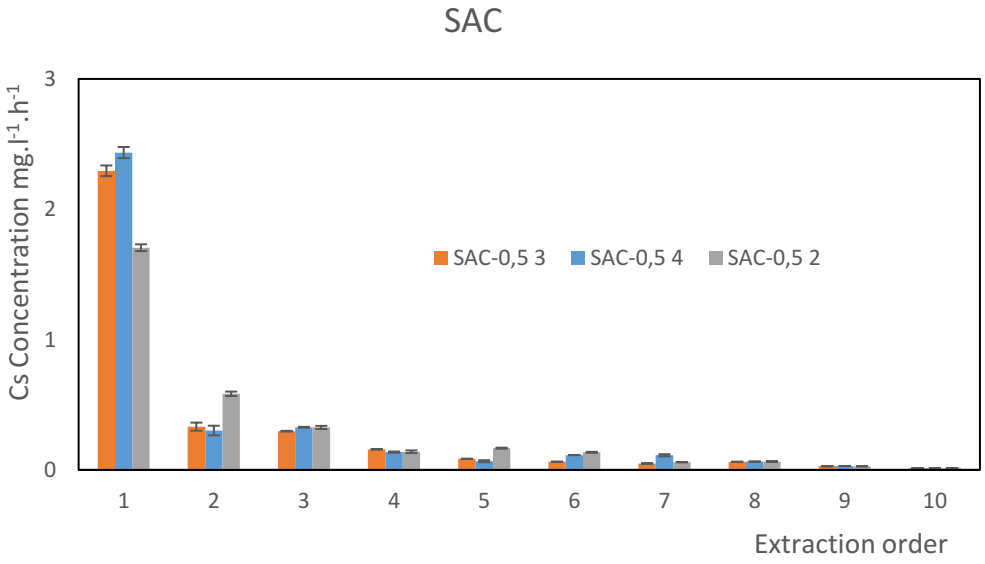

Figure 5.7. Concentration of Cs in group SAC, divided by the number of hours of extraction length. Beam height was set to 4 mm, air flow rate 72 mL·s^{-1}, acetylene flow rate at 24 mL·s^{-1}.

HCl was operated at a lamp current of 15.0 mA and a wavelength of 852.1 nm. Table of results is attached in appendix A in table 4, 5 and 6.

5.3.2. Results of extracts with ionization buffer

In groups with added ionization buffer (figure 5.8., figure 5.9., figure 5.10., figure 5.11., figure 5.12., figure 5.13.), we can observe similar trends as without the addition of ionization buffer. Differences in concentration of Cs in some extracts (NP-0,5 3, NP-M-0,5 3, NP-M-0,5 2, NP-Z-0,5 2) could be explained by ionization of the analyte during measurement without the ionization buffer. This would prove the requirement of addition of ionization buffer.

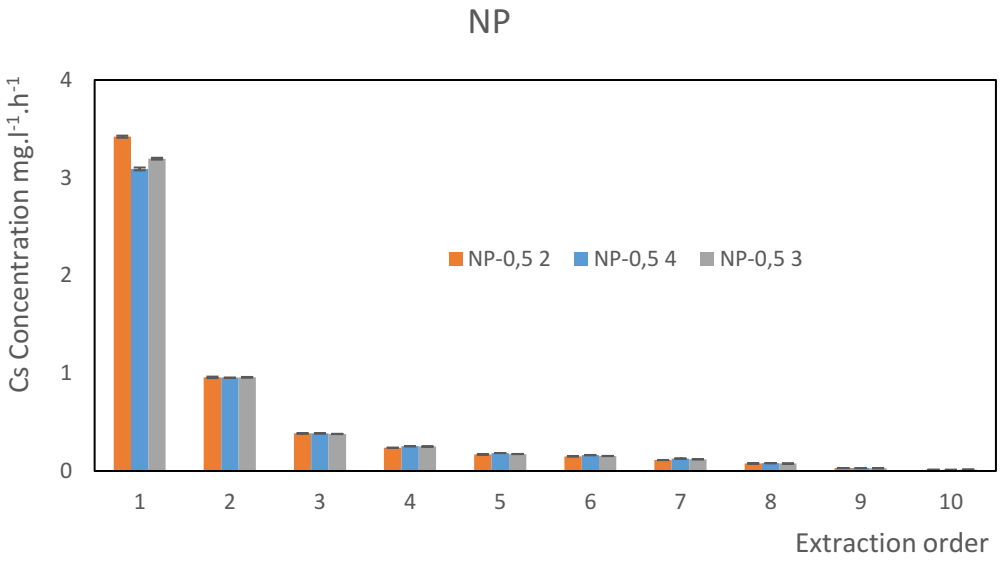

Figure 5.8. Concentration of Cs in group NP + KCl, divided by the number of hours of extraction length. Beam height was set to 4 mm, air flow rate 72 mL·s^{-1}, acetylene flow rate at 24 mL·s^{-1}. HCl was operated at a lamp current of 15.0 mA and a wavelength of 852.1 nm. Table of results is attached in appendix A in table 18, 19 and 20.

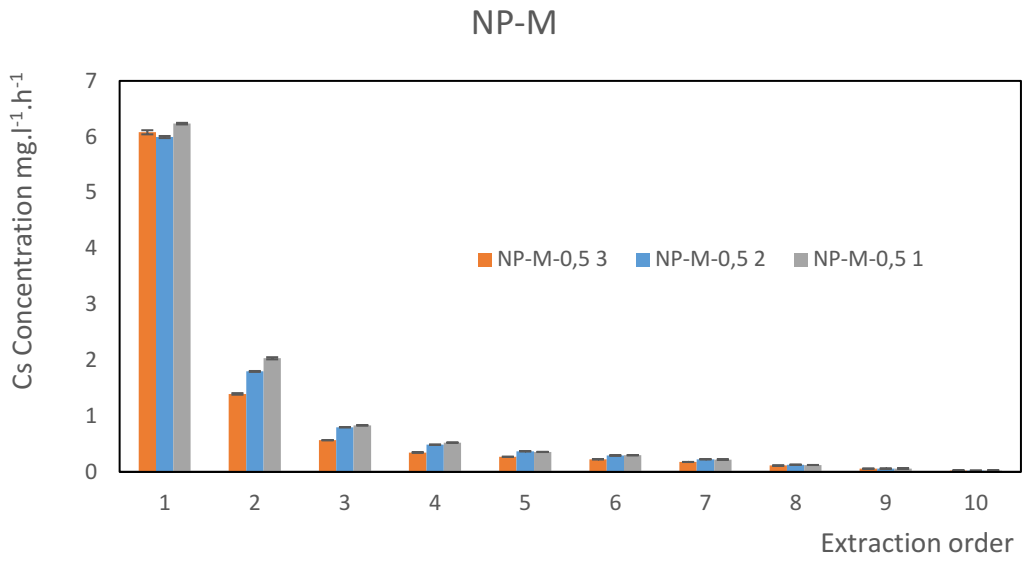

Figure 5.9. Concentration of Cs in group NP-M + KCl, divided by the number of hours of extraction length. Beam height was set to 4 mm, air flow rate 72 mL·s^{-1}, acetylene flow rate at 24 mL·s^{-1}. HCl was operated at a lamp current of 15.0 mA and a wavelength of 852.1 nm. Table of results is attached in appendix A in table 27, 28 and 29.

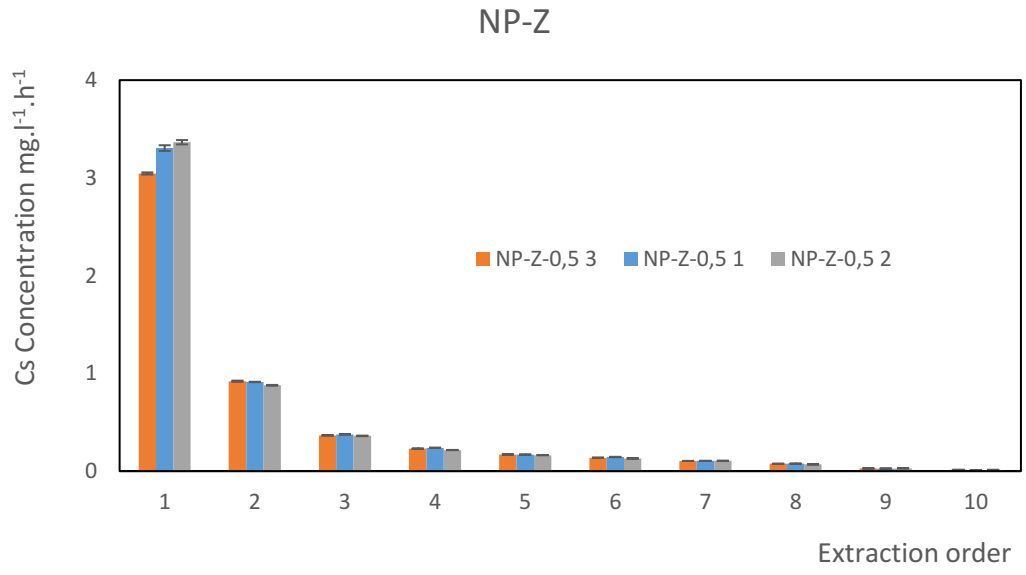

Figure 5.10. Concentration of Cs in group NP-Z + KCl, divided by the number of hours of extraction length. Beam height was set to 4 mm, air flow rate 72 mL·s^{-1}, acetylene flow rate at

24 mL·s^{-1}. HCl was operated at a lamp current of 15.0 mA and a wavelength of 852.1 nm. Table of results is attached in appendix A in table 30, 31 and 32.

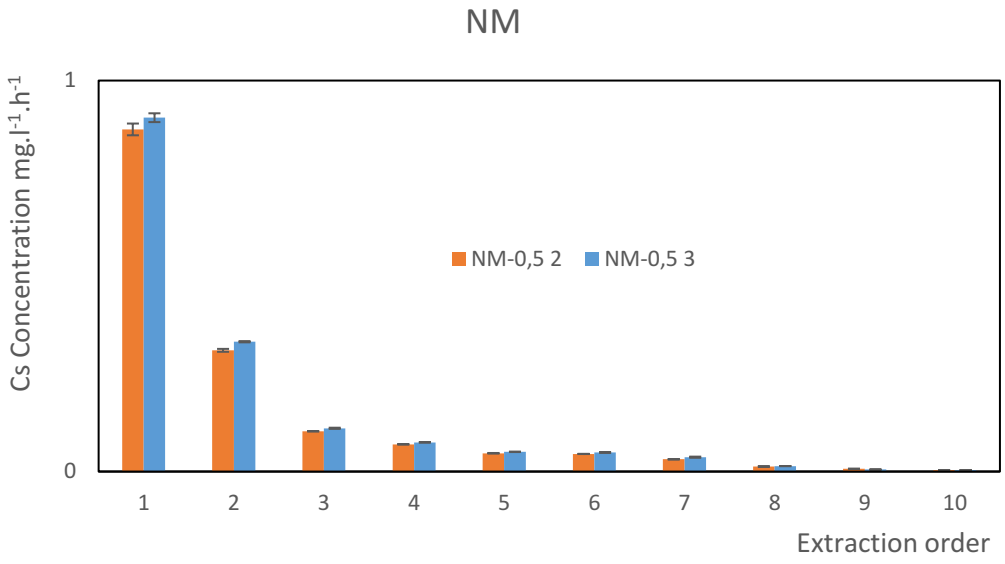

Figure 5.11. Concentration of Cs in group NM + KCl, divided by the number of hours of extraction length. Beam height was set to 4 mm, air flow rate 72 mL·s^{-1}, acetylene flow rate at 24 mL·s^{-1}. HCl was operated at a lamp current of 15.0 mA and a wavelength of 852.1 nm. Table of results is attached in appendix A in table 33 and 34.

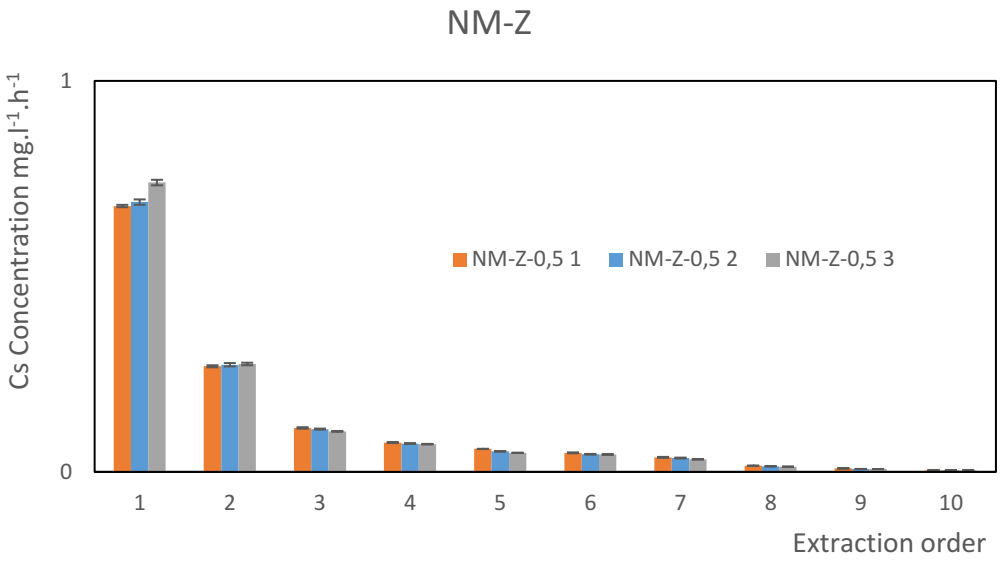

Figure 5.12. Concentration of Cs in group NM-Z + KCl, divided by the number of hours of extraction length. Beam height was set to 4 mm, air flow rate 72 mL·s^{-1}, acetylene flow rate at 24 mL·s^{-1}. HCl was operated at a lamp current of 15.0 mA and a wavelength of 852.1 nm. Table of results is attached in appendix A in table 24, 25 and 26.

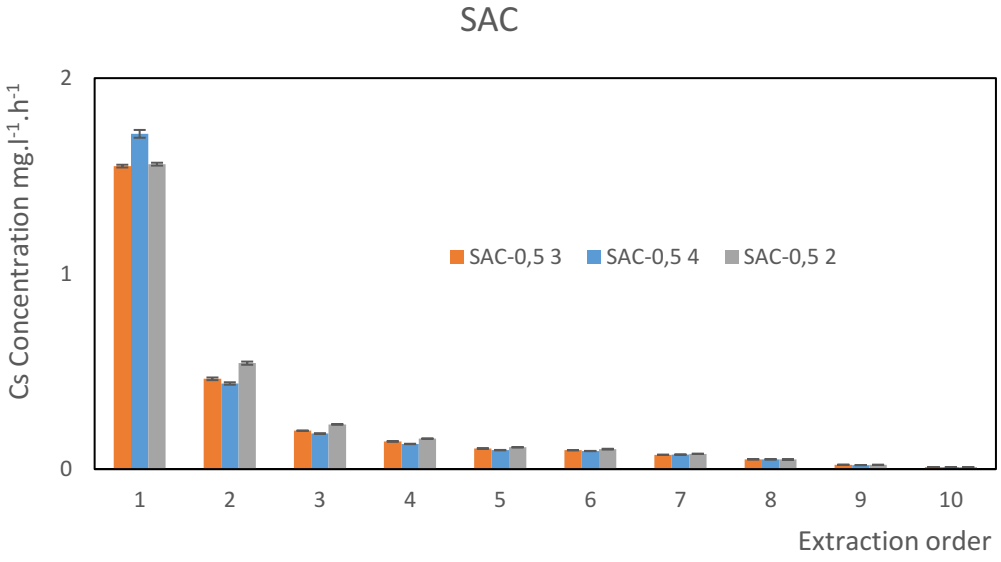

Figure 5.13. Concentration of Cs in group SAC + KCl, divided by the number of hours of extraction length. Beam height was set to 4 mm, air flow rate 72 mL·s^{-1}, acetylene flow rate at

24 $mL \cdot s^{-1}$. HCl was operated at a lamp current of 15.0 mA and a wavelength of 852.1 nm. Table of results is attached in appendix A in table 21, 22 and 23.

6. Conclusions

Seventeen cement samples were acquired from CTU as a model samples for radioactive waste, containing nonradioactive nuclides of Cs, widely used for waste storage in the ground. Out of each of the sample, ten extractions with water were made, with extraction time ranging from 2 to 1036 hours. Influence of deionized or distilled water source on Cs concentration in extracts was questioned and dismissed. Cs content in these extracts was determined using F-AAS method, chosen for its suitability and practicality. Beam height and acetylene flow rate for F-AAS method for determination of Cs in water extracts was optimized. Optimal beam height was measured to be 4 mm and acetylene flow rate 24 $mL \cdot s^{-1}$. Limit of detection was calculated at 0.116 $mg \cdot L^{-1}$ and limit of quantification was determined 0.386 $mg \cdot L^{-1}$. Addition of ionization buffer to the extracts was explored and compared with results without the addition of ionization buffer, with differences found in concentration levels of some extracts, proving the need for addition of ionization buffer.

7. References

[1] Gauglitz G., Vo-Dinh T., Handbook of Spectroscopy Volume 1, Weinheim, WILEY-VCH (2003).

[2] Greenwood N.N., Earnshaw A., Chemie prvků. Praha, Informatorium, (1993).

[3] Housecroft, C. E., Anorganická chemie, Praha, Vysoká škola chemicko-technologická, (2014).

[4] Shriver, D. F., Atkins, P. W., Inorganic chemistry, Oxford, Oxford University Press, (1999).

[5] Toužín, J., Stručný přehled chemie prvků, Brno, Masarykova Univerzita, (2003).

[6] Tokalioğlu, Ş., Kartal, Ş., & Elçi, L., Determination of heavy metals and their speciation in lake sediments by flame atomic absorption spectrometry after a four-stage sequential extraction procedure, Analytica Chimica Acta, 413(1-2), 33–40, (2000).

[7] Vinichuk, M., Taylor, A. F. S., Rosén, K., Johanson, K. J., Accumulation of potassium, rubidium and caesium (133Cs and 137Cs) in various fractions of soil and fungi in a Swedish forest, Science of The Total Environment, 408(12), 2543–2548. (2010).

[8] Roulier, M., Bueno, M., Coppin, F., Nicolas, M., Thiry, Y., Rigal, F., Le Hécho, I., Atmospheric iodine, selenium and caesium depositions in France: II. Influence of forest canopies, Chemosphere, 128952, (2020).

[9] Mohanrao, G. J., Folsom, T. R., Gamma-ray spectrometric determination of low concentrations of radioactive caesium in sea water by a nickel ferrocyanide method, The Analyst, 88(1043), 105, (1963).

[10] Duckworth, A., Adrain, R. S., Tozer, B. A., Detection of laser-ablated caesium atoms with resonance ionization and time-of-flight mass spectrometry, Journal of Physics D: Applied Physics, 24(11), 1925–1932, (1991).

[11] Groll, H., Niemax, K., Multielement diode laser atomic absorption spectrometry in graphite tube furnaces and analytical flames, Spectrochimica Acta Part B: Atomic Spectroscopy, 48(5), 633–641, (1993).

[12] Townshend, A., Encyclopedia of analytical science. Vol. 7, London, Academic Press, (1995).

[13] Frigieri, P., Trucco, R., Ciaccolini, I., Pampurini, G., Determination of caesium in river and sea waters by electrothermal atomic-absorption spectrometry, Interference of cobalt and iron, The Analyst, 105(1252), 651, (1980).

[14] Anderson, P., Davidson, C. M., Littlejohn, D., Ure, A. M., Shand, C. A., Cheshire, M. V., The determination of caesium and silver in soil and fungal fruiting bodies by electrothermal atomic absorption spectrometry, Analytica Chimica Acta, 327(1), 53–60, (1996).

[15] Grobenski, Z., Weber, D., Welz, B., Wolff, J., Determination of caesium and rubidium by flame and furnace atomic-absorption spectrometry, The Analyst, 108(1289), 925, (1983).

[16] Skoog, D. A., West, D. M., Holler, F. J., Crouch, S. R., Analytická chemie, Praha, Vysoká škola chemicko-technologická, (2019).

[17] Záruba, K., Analytická chemie. (2. díl), Praha, Vysoká škola chemicko-technologická v Praze, (2016).

[18] Kellner R., Mermet J.–M., Otto M., Varcárcel M., Widmer H. M., Analytical chemistry: a modern approach to analytical science. Second edition. Weinheim, Wiley-VCH, (2004).

[19] https://www.wikiwand.com/en/Atomic_absorption_spectroscopy (27.3.2021).

[20] García, R., Báez, A. P., Atomic absorption spectrometry (AAS), Atomic absorption spectroscopy, 1: 1-13. (2012).

[21] Atomic Absorption. Redefined. contrAA800, Analytik Jena GmbH, (2020).

[22] Shrader D., Moffett J., Plant G., Sturman B., Sullivan J. V., Hamme L., Practical Multi-Element Hollow Cathode Lamps for Atomic Absorption Spectrometry https://www.agilent.com/cs/library/applications/a-aa09.pdf (21.8.2021).

[23] Gauglitz G., Moore D. S., Handbook of spectroscopy. 2nd, compl. rev. and enlarged ed., Weinheim, Wiley-VCH, (2014).

[24] Higson, S. P. J., Analytical chemistry, Oxford, Oxford University Press, (2004).

[25] Glasser, F., Application of inorganic cements to the conditioning and immobilisation of radioactive wastes, Handbook of Advanced Radioactive Waste Conditioning Technologies, 67–135, (2011).

[26] Atkins, M., Glasser, F. P., Application of portland cement-based materials to radioactive waste immobilization, Waste Management 12(2-3), 105–131, (1992).

[27] Siddique, R., & Klaus, J., Influence of metakaolin on the properties of mortar and concrete: A review, Applied Clay Science, 43(3-4), 392–400, (2009).

[28] Elkamash, A., Enaggar, M., Eldessouky, M., Immobilization of cesium and strontium radionuclides in zeolite-cement blends, Journal of Hazardous Materials, 136(2), 310–316, (2006).

[29] García-Gutiérrez, M., Missana, T., Mingarro, M., Morejón, J., & Cormenzana, J. L., Cesium diffusion in mortars from different cements used in radioactive waste repositories, Applied Geochemistry, 98, 10–16, (2018).

[30] Rehab O. Abdel Rahman, Michael I. Ojovan, Sustainability of Life Cycle Management for Nuclear Cementation-Based Technologies, Woodhead Publishing, 181-232, (2021).
[31] Li ZJ, Advanced Concrete Technology, John Wiley & Sons, Inc. (2011).
[32] Li, L., Easterbrook, D., Xia, J., Jin, W. L., Numerical simulation of chloride penetration in concrete in rapid chloride migration tests, Cement and Concrete Composites, 63, 113–121, (2015).
[33] Jenni, A., Hyatt, N. C., Encapsulation of caesium-loaded Ionsiv in cement, Cement and Concrete Research, 40(8), 1271–1277, (2010).
[34] de Almeida Calábria, J. A., Cota, S. D. S., de Morais, G. F., Ladeira, A. C. Q., Impact of alkaline alterations to a Brazilian soil on cesium retention under low temperature conditions, Journal of Environmental Radioactivity, 178-179, 95–100, (2017).
[35] Dyer, A., Chow, J. K. K., The uptake of radioisotopes onto clays and other natural materials, Journal of Radioanalytical and Nuclear Chemistry, 242(2), 321–328, (1999).
[36] Reynier, N., Lastra, R., Laviolette, C., Fiset, J.-F., Bouzoubaâ, N., Chapman, M., Uranium, Cesium, and Mercury Leaching and Recovery from Cemented Radioactive Wastes in Sulfuric Acid and Iodide Media, Minerals, 5(4), 744–757, (2015).
[37] Plecas, I., Peric, A., Kostadinovic, A., Drljaca, J., Glodic, S., Leaching behavior of 60Co and 173Cs from spent ion exchange resins in cement matrix, Cement and Concrete Research, 22(5), 937–940. doi:10.1016/0008-8846(92)90117-e, (1992).
[38] Nishi, T., Matsuda, M., Chino, K., Kikuchi, M., Reduction of cesium leachability from cementitous resin forms using natural acid clay and zeolite, Cement and Concrete Research, 22(2-3), 387–392. doi:10.1016/0008-8846(92)90080-f, (1992).
[39] Szalo, A., Žatkulák, M., Borate Compound Content Reduction in Liquid Radioactive Waste From Nuclear Power Plants With VVER Reactor, Nuclear Energy in Central Europe, 1-6, (2000).
[40] Koťátková, J., Zatloukal, J., Reiterman, P., Kolář, K., Concrete and cement composites used for radioactive waste deposition, Journal of Environmental Radioactivity, ISSN 18791700, 178–179, 147–155, (2017).
[41] Koťátková, J., Zatloukal, J., Kolář, K., Mechanical and setting/hardening conditions of cement pastes for evaporator concentrates incorporating admixtures, International Conference of Numerical Analysis and Applied Mathematics ICNAAM, AIP Publishing, p. 070004, (2019).

[42] Zatloukalová, J., Dewynter-Marty, V., Zatloukal, J., Kolář, K., Bernachy-Barbe, F., Bezdička, P., Konvalinka, P., Microstructural and micro-mechanical property changes of cement pastes for ILW immobilization due to irradiation, Journal of Nuclear Materials, 540, (2020).

[43] Zatloukalová, J., Dewynter-Marty, V., Zatloukal, J., Kolář, K., Hlaváč, Z., Konvalinka, P., Mechanical properties of irradiated cement pastes for immobilization of evaporator concentrates, Progress in Nuclear Energy, 127, (2020).

[44] Zatloukalová, J., Dewynter-Marty, V., Zatloukal, J., Kolář, K., Hlaváč, Z., Guillot W., Konvalinka, P., Investigation of radiolysis in cement pastes immobilizing simulated evaporator concrentrates, Annals of Nuclear Energy, 151, (2021).

[45] El-Kamash, A., El-Dakroury, A., & Aly, H., Leaching kinetics of 137Cs and 60Co radionuclides fixed in cement and cement-based materials, Cement and Concrete Research, 32(11), 1797–1803, (2002).

[46] Welz B., Sperling M., Atomic Absorption Spectrometry (3rd edn.), Weinheim, Wiley - VCH, 360-361, (1999).

[47] Watling, R. J., Watling, H. R., A modified branched capillary for ionization suppression in AAS, Spectrochimica Acta Part B: Atomic Spectroscopy, 37(7), 633–636, (1982).

[48] Kornblum, G. R., De Galan L., Ionization interference in the acetylene-nitrous oxide flame, Spectrochimica Acta Part B: Atomic Spectroscopy 28.4, 139-147, (1973).

[49] Hill, S. J., ATOMIC ABSORPTION SPECTROMETRY | Flame, Reference Module in Chemistry, Molecular Sciences and Chemical Engineering, (2013).

[50] Lyra, F. H., et al., Determination of Na, K, Ca and Mg in biodiesel samples by flame atomic absorption spectrometry (F AAS) using microemulsion as sample preparation, Microchemical Journal 96.1, 180-185, (2010).

Appendix A

Results of determination of Cs in extraction samples.

Table 1. Results of Cs concentration for sample NP-0,5 3 from sample group NP without the addition of ionization buffer.

Number of extraction	Duration of extraction [h]	Concentration [$mg \cdot L^{-1}$]	ASD	Concentration divided by extraction length [$mg \cdot L^{-1} \cdot h^{-1}$]
1	2	7.98	0.12	3.99
2	5	5.36	0.10	1.07
3	17	8.82	0.14	0.52
4	24	5.95	0.21	0.25
5	24	6.06	0.06	0.25
6	24	5.09	0.01	0.21
7	24	2.32	0.09	0.10
8	336	13.72	0.83	0.04
9	672	26.95	0.07	0.04
10	1032	19.35	0.10	0.02

Table 2. Results of Cs concentration for sample NP-0,5 2 from sample group NP without the addition of ionization buffer.

Number of extraction	Duration of extraction [h]	Concentration [$mg \cdot L^{-1}$]	ASD	Concentration divided by extraction length [$mg \cdot L^{-1} \cdot h^{-1}$]
1	2	8.78	0.03	4.39
2	5	5.71	0.11	1.14
3	17	9.63	0.36	0.57
4	24	7.10	0.03	0.30
5	24	5.83	0.06	0.24
6	24	2.63	0.32	0.11
7	24	2.11	0.18	0.09
8	336	29.85	0.28	0.09
9	672	26.13	0.24	0.04
10	1032	17.79	0.15	0.02

Table 3. Results of Cs concentration for sample NP-0,5 4 from sample group NP without the addition of ionization buffer.

Number of extraction	Duration of extraction [h]	Concentration [$mg \cdot L^{-1}$]	ASD	Concentration divided by extraction length [$mg \cdot L^{-1} \cdot h^{-1}$]
1	2	7.74	0.07	3.87
2	5	6.29	0.04	1.26
3	17	10.92	0.08	0.64
4	24	7.48	0.12	0.31
5	24	4.36	0.08	0.18
6	24	3.76	0.41	0.16
7	24	4.61	0.11	0.19
8	336	30.02	0.88	0.09
9	672	27.15	0.12	0.04
10	1032	18.66	0.15	0.02

Table 4. Results of Cs concentration for sample SAC-0,5 3 from sample group SAC without the addition of ionization buffer.

Number of extraction	Duration of extraction [h]	Concentration [$mg \cdot L^{-1}$]	ASD	Concentration divided by extraction length [$mg \cdot L^{-1} \cdot h^{-1}$]
1	2	4.59	0.08	2.30
2	5	1.66	0.16	0.33
3	17	5.05	0.05	0.30
4	24	3.79	0.02	0.16
5	24	2.04	0.00	0.09
6	24	1.50	0.00	0.06
7	24	1.18	0.00	0.05
8	336	20.87	0.10	0.06
9	672	18.89	0.10	0.03
10	1032	14.31	0.34	0.01

Table 5. Results of Cs concentration for sample SAC-0,5 4 from sample group SAC without the addition of ionization buffer.

Number of extraction	Duration of extraction [h]	Concentration [$mg \cdot L^{-1}$]	ASD	Concentration divided by extraction length [$mg \cdot L^{-1} \cdot h^{-1}$]
1	2	4.87	0.09	2.44
2	5	1.51	0.19	0.30
3	17	5.56	0.05	0.33
4	24	3.27	0.11	0.14
5	24	1.60	0.19	0.07
6	24	2.73	0.02	0.11
7	24	2.69	0.20	0.11
8	336	21.21	0.11	0.06
9	672	20.17	0.05	0.03
10	1032	13.00	0.09	0.01

Table 6. Results of Cs concentration for sample SAC-0,5 2 from sample group SAC without the addition of ionization buffer.

Number of extraction	Duration of extraction [h]	Concentration [$mg \cdot L^{-1}$]	ASD	Concentration divided by extraction length [$mg \cdot L^{-1} \cdot h^{-1}$]
1	2	3.41	0.05	1.71
2	5	2.92	0.08	0.58
3	17	5.54	0.20	0.33
4	24	3.35	0.24	0.14
5	24	4.00	0.09	0.17
6	24	3.23	0.09	0.13
7	24	1.42	0.00	0.06
8	336	21.61	0.25	0.06
9	672	18.79	0.14	0.03
10	1032	13.89	0.08	0.01

Table 7. Results of Cs concentration for sample NM-Z-0,5 1 from sample group NM-Z without the addition of ionization buffer.

Number of extraction	Duration of extraction [h]	Concentration [$mg \cdot L^{-1}$]	ASD	Concentration divided by extraction length [$mg \cdot L^{-1} \cdot h^{-1}$]
1	2	1.98	0.14	0.99
2	5	1.72	0.19	0.34
3	17	1.82	0.21	0.11
4	24	2.78	0.14	0.12
5	24	2.71	0.22	0.11
6	24	1.33	0.03	0.06
7	24	0.99	0.13	0.04
8	336	7.66	0.12	0.02
9	672	6.82	0.03	0.01
10	1032	5.49	0.31	0.01

Table 8. Results of Cs concentration for sample NM-Z-0,5 2 from sample group NM-Z without the addition of ionization buffer.

Number of extraction	Duration of extraction [h]	Concentration [$mg \cdot L^{-1}$]	ASD	Concentration divided by extraction length [$mg \cdot L^{-1} \cdot h^{-1}$]
1	2	2.19	0.04	1.10
2	5	2.02	0.01	0.40
3	17	1.68	0.16	0.10
4	24	2.40	0.16	0.10
5	24	0.33	0.00	0.01
6	24	0.84	0.00	0.04
7	24	0.29	0.00	0.01
8	336	5.78	0.30	0.02
9	672	5.45	0.27	0.01
10	1032	5.83	0.02	0.01

Table 9. Results of Cs concentration for sample NM-Z-0,5 3 from sample group NM-Z without the addition of ionization buffer.

Number of extraction	Duration of extraction [h]	Concentration [$mg \cdot L^{-1}$]	ASD	Concentration divided by extraction length [$mg \cdot L^{-1} \cdot h^{-1}$]
1	2	2.90	0.03	1.45
2	5	1.35	0.19	0.27
3	17	2.75	0.13	0.16
4	24	2.81	0.02	0.12
5	24	1.68	0.11	0.07
6	24	1.24	0.04	0.05
7	24	0.10	0.00	0.00
8	336	5.16	0.20	0.02
9	672	5.45	0.09	0.01
10	1032	4.52	0.19	0.00

Table 10. Results of Cs concentration for sample NP-M-0,5 3 from sample group NP-M without the addition of ionization buffer.

Number of extraction	Duration of extraction [h]	Concentration [$mg \cdot L^{-1}$]	ASD	Concentration divided by extraction length [$mg \cdot L^{-1} \cdot h^{-1}$]
1	2	16.48	0.04	8.24
2	5	9.11	0.06	1.82
3	17	13.96	0.04	0.82
4	24	10.54	0.12	0.44
5	24	7.74	0.28	0.32
6	24	6.53	0.05	0.27
7	24	6.04	0.09	0.25
8	336	1.52	0.02	0.00
9	672	46.41	1.05	0.07
10	1032	27.68	0.78	0.03

Table 11. Results of Cs concentration for sample NP-M-0,5 2 from sample group NP-M without the addition of ionization buffer.

Number of extraction	Duration of extraction [h]	Concentration [$mg \cdot L^{-1}$]	ASD	Concentration divided by extraction length [$mg \cdot L^{-1} \cdot h^{-1}$]
1	2	16.88	0.10	8.44
2	5	12.34	0.15	2.47
3	17	18.87	0.28	1.11
4	24	13.29	0.33	0.55
5	24	11.98	0.08	0.50
6	24	7.07	0.39	0.29
7	24	7.51	0.09	0.31
8	336	1.31	0.12	0.00
9	672	39.88	1.44	0.06
10	1032	14.45	2.03	0.01

Table 12. Results of Cs concentration for sample NP-M-0,5 1 from sample group NP-M without the addition of ionization buffer.

Number of extraction	Duration of extraction [h]	Concentration [$mg \cdot L^{-1}$]	ASD	Concentration divided by extraction length [$mg \cdot L^{-1} \cdot h^{-1}$]
1	2	18.20	0.03	9.10
2	5	12.84	0.27	2.57
3	17	19.31	0.07	1.14
4	24	13.82	0.14	0.58
5	24	11.57	0.04	0.48
6	24	9.16	0.08	0.38
7	24	7.62	0.13	0.32
8	336	36.61	0.72	0.11
9	672	45.15	1.57	0.07
10	1032	27.66	1.19	0.03

Table 13. Results of Cs concentration for sample NP-Z-0,5 3 from sample group NP-Z without the addition of ionization buffer.

Number of extraction	Duration of extraction [h]	Concentration [$mg \cdot L^{-1}$]	ASD	Concentration divided by extraction length [$mg \cdot L^{-1} \cdot h^{-1}$]
1	2	9.13	0.17	4.57
2	5	5.41	0.10	1.08
3	17	9.77	0.09	0.57
4	24	6.20	0.17	0.26
5	24	4.73	0.16	0.20
6	24	2.86	0.34	0.12
7	24	3.41	0.16	0.14
8	336	25.56	1.18	0.08
9	672	24.88	0.11	0.04
10	1032	19.37	0.24	0.02

Table 14. Results of Cs concentration for sample NP-Z-0,5 1 from sample group NP-Z without the addition of ionization buffer.

Number of extraction	Duration of extraction [h]	Concentration [$mg \cdot L^{-1}$]	ASD	Concentration divided by extraction length [$mg \cdot L^{-1} \cdot h^{-1}$]
1	2	9.47	0.06	4.74
2	5	6.33	0.11	1.27
3	17	10.45	0.08	0.61
4	24	6.13	0.05	0.26
5	24	3.76	0.09	0.16
6	24	3.17	0.37	0.13
7	24	3.18	0.25	0.13
8	336	28.21	0.30	0.08
9	672	24.48	0.10	0.04
10	1032	18.51	0.04	0.02

Table 15. Results of Cs concentration for sample NP-0,5 2 from sample group NP-Z without the addition of ionization buffer.

Number of extraction	Duration of extraction [h]	Concentration [$mg \cdot L^{-1}$]	ASD	Concentration divided by extraction length [$mg \cdot L^{-1} \cdot h^{-1}$]
1	2	9.64	0.08	4.82
2	5	6.01	0.09	1.20
3	17	8.88	0.15	0.52
4	24	6.69	0.08	0.28
5	24	6.26	0.05	0.26
6	24	2.32	0.34	0.10
7	24	2.28	0.22	0.10
8	336	7.80	0.00	0.02
9	672	24.35	0.14	0.04
10	1032	19.06	0.09	0.02

Table 16. Results of Cs concentration for sample NM-0,5 2 from sample group NM without the addition of ionization buffer.

Number of extraction	Duration of extraction [h]	Concentration [$mg \cdot L^{-1}$]	ASD	Concentration divided by extraction length [$mg \cdot L^{-1} \cdot h^{-1}$]
1	2	1.91	0.06	0.96
2	5	1.62	0.06	0.32
3	17	3.83	0.12	0.23
4	24	0.49	0.00	0.02
5	24	1.66	0.11	0.07
6	24	1.15	0.16	0.05
7	24	0.69	0.00	0.03
8	336	4.85	0.30	0.01
9	672	5.67	0.09	0.01
10	1032	5.56	0.03	0.01

Table 17. Results of Cs concentration for sample NM-0,5 3 from sample group NM without the addition of ionization buffer.

Number of extraction	Duration of extraction [h]	Concentration [$mg \cdot L^{-1}$]	ASD	Concentration divided by extraction length [$mg \cdot L^{-1} \cdot h^{-1}$]
1	2	2.36	0.03	1.18
2	5	1.21	0.00	0.24
3	17	2.65	0.22	0.16
4	24	1.49	0.00	0.06
5	24	0.30	0.00	0.01
6	24	1.55	0.05	0.06
7	24	1.68	0.08	0.07
8	336	5.04	0.08	0.02
9	672	6.27	0.11	0.01
10	1032	4.51	0.08	0.00

Table 18. Results of Cs concentration for sample NP-0,5 2 from sample group NP + KCl with the addition of ionization buffer KCl.

Number of extraction	Duration of extraction [h]	Concentration [$mg \cdot L^{-1}$]	ASD	Concentration divided by extraction length [$mg \cdot L^{-1} \cdot h^{-1}$]
1	2	6.84	0.02	3.42
2	5	4.79	0.04	0.96
3	17	6.53	0.02	0.38
4	24	5.70	0.04	0.24
5	24	4.06	0.01	0.17
6	24	3.60	0.03	0.15
7	24	2.68	0.02	0.11
8	336	25.79	0.06	0.08
9	672	20.44	0.16	0.03
10	1032	12.86	0.23	0.01

Table 19. Results of Cs concentration for sample NP-0,5 4 from sample group NP + KCl with the addition of ionization buffer KCl.

Number of extraction	Duration of extraction [h]	Concentration [$mg \cdot L^{-1}$]	ASD	Concentration divided by extraction length [$mg \cdot L^{-1} \cdot h^{-1}$]
1	2	6.18	0.03	3.09
2	5	4.77	0.01	0.95
3	17	6.54	0.06	0.38
4	24	6.07	0.04	0.25
5	24	4.40	0.02	0.18
6	24	3.89	0.05	0.16
7	24	3.04	0.01	0.13
8	336	26.80	0.14	0.08
9	672	20.32	0.04	0.03
10	1032	12.43	0.18	0.01

Table 20. Results of Cs concentration for sample NP-0,5 3 from sample group NP + KCl with the addition of ionization buffer KCl.

Number of extraction	Duration of extraction [h]	Concentration [$mg \cdot L^{-1}$]	ASD	Concentration divided by extraction length [$mg \cdot L^{-1} \cdot h^{-1}$]
1	2	6.39	0.02	3.20
2	5	4.79	0.02	0.96
3	17	6.44	0.03	0.38
4	24	6.00	0.02	0.25
5	24	4.16	0.02	0.17
6	24	3.68	0.02	0.15
7	24	2.87	0.03	0.12
8	336	25.45	0.19	0.08
9	672	19.03	0.31	0.03
10	1032	14.27	0.05	0.01

Table 21. Results of Cs concentration for sample SAC-0,5 3 from sample group SAC + KCl with the addition of ionization buffer KCl.

Number of extraction	Duration of extraction [h]	Concentration [$mg \cdot L^{-1}$]	ASD	Concentration divided by extraction length [$mg \cdot L^{-1} \cdot h^{-1}$]
1	2	3.10	0.01	1.55
2	5	2.31	0.03	0.46
3	17	3.34	0.01	0.20
4	24	3.40	0.01	0.14
5	24	2.53	0.02	0.11
6	24	2.32	0.01	0.10
7	24	1.76	0.02	0.07
8	336	16.83	0.04	0.05
9	672	14.98	0.07	0.02
10	1032	11.00	0.06	0.01

Table 22. Results of Cs concentration for sample SAC-0,5 4 from sample group SAC + KCl with the addition of ionization buffer KCl.

Number of extraction	Duration of extraction [h]	Concentration [$mg \cdot L^{-1}$]	ASD	Concentration divided by extraction length [$mg \cdot L^{-1} \cdot h^{-1}$]
1	2	3.43	0.04	1.72
2	5	2.19	0.03	0.44
3	17	3.09	0.02	0.18
4	24	3.09	0.03	0.13
5	24	2.33	0.03	0.10
6	24	2.22	0.02	0.09
7	24	1.78	0.01	0.07
8	336	16.81	0.04	0.05
9	672	13.79	0.17	0.02
10	1032	10.35	0.11	0.01

Table 23. Results of Cs concentration for sample SAC-0,5 2 from sample group SAC + KCl with the addition of ionization buffer KCl.

Number of extraction	Duration of extraction [h]	Concentration [$mg \cdot L^{-1}$]	ASD	Concentration divided by extraction length [$mg \cdot L^{-1} \cdot h^{-1}$]
1	2	3.12	0.01	1.56
2	5	2.71	0.04	0.54
3	17	3.89	0.03	0.23
4	24	3.74	0.04	0.16
5	24	2.68	0.03	0.11
6	24	2.45	0.05	0.10
7	24	1.88	0.02	0.08
8	336	16.51	0.03	0.05
9	672	14.77	0.13	0.02
10	1032	10.58	0.16	0.01

Table 24. Results of Cs concentration for sample NM-Z-0,5 1 from sample group NM-Z + KCl with the addition of ionization buffer KCl.

Number of extraction	Duration of extraction [h]	Concentration [$mg \cdot L^{-1}$]	ASD	Concentration divided by extraction length [$mg \cdot L^{-1} \cdot h^{-1}$]
1	2	1.36	0.01	0.68
2	5	1.35	0.01	0.27
3	17	1.91	0.03	0.11
4	24	1.80	0.03	0.08
5	24	1.41	0.01	0.06
6	24	1.17	0.03	0.05
7	24	0.89	0.03	0.04
8	336	5.27	0.00	0.02
9	672	5.97	0.06	0.01
10	1032	4.35	0.04	0.00

Table 25. Results of Cs concentration for sample NM-Z-0,5 2 from sample group NM-Z + KCl with the addition of ionization buffer KCl.

Number of extraction	Duration of extraction [h]	Concentration [mg·L^{-1}]	ASD	Concentration divided by extraction length [mg·L^{-1}·h^{-1}]
1	2	1.38	0.01	0.69
2	5	1.37	0.02	0.27
3	17	1.86	0.02	0.11
4	24	1.74	0.02	0.07
5	24	1.26	0.01	0.05
6	24	1.08	0.02	0.05
7	24	0.85	0.03	0.04
8	336	4.78	0.04	0.01
9	672	4.98	0.13	0.01
10	1032	4.01	0.12	0.00

Table 26. Results of Cs concentration for sample NM-Z-0,5 3 from sample group NM-Z + KCl with the addition of ionization buffer KCl.

Number of extraction	Duration of extraction [h]	Concentration [mg·L^{-1}]	ASD	Concentration divided by extraction length [mg·L^{-1}·h^{-1}]
1	2	1.48	0.01	0.74
2	5	1.38	0.02	0.28
3	17	1.76	0.00	0.10
4	24	1.70	0.02	0.07
5	24	1.17	0.01	0.05
6	24	1.07	0.02	0.04
7	24	0.77	0.00	0.03
8	336	4.47	0.06	0.01
9	672	4.87	0.05	0.01
10	1032	3.72	0.05	0.00

Table 27. Results of Cs concentration for sample NP-M-0,5 3 from sample group NP-M + KCl with the addition of ionization buffer KCl.

Number of extraction	Duration of extraction [h]	Concentration [mg·L^{-1}]	ASD	Concentration divided by extraction length [mg·L^{-1}·h^{-1}]
1	2	12.16	0.07	6.08
2	5	6.98	0.07	1.40
3	17	9.64	0.02	0.57
4	24	8.34	0.05	0.35
5	24	6.49	0.02	0.27
6	24	5.41	0.03	0.23
7	24	4.26	0.03	0.18
8	336	37.95	0.26	0.11
9	672	38.72	0.14	0.06
10	1032	26.41	0.16	0.03

Table 28. Results of Cs concentration for sample NP-M-0,5 2 from sample group NP-M + KCl with the addition of ionization buffer KCl.

Number of extraction	Duration of extraction [h]	Concentration [mg·L^{-1}]	ASD	Concentration divided by extraction length [mg·L^{-1}·h^{-1}]
1	2	11.99	0.04	6.00
2	5	8.99	0.04	1.80
3	17	13.58	0.08	0.80
4	24	11.69	0.10	0.49
5	24	8.86	0.03	0.37
6	24	7.05	0.02	0.29
7	24	5.42	0.03	0.23
8	336	43.20	0.32	0.13
9	672	39.32	0.20	0.06
10	1032	23.12	0.26	0.02

Table 29. Results of Cs concentration for sample NP-M-0,5 1 from sample group NP-M + KCl with the addition of ionization buffer KCl.

Number of extraction	Duration of extraction [h]	Concentration [mg·L^{-1}]	ASD	Concentration divided by extraction length [mg·L^{-1}·h^{-1}]
1	2	12.47	0.03	6.24
2	5	10.17	0.10	2.03
3	17	14.16	0.08	0.83
4	24	12.58	0.01	0.52
5	24	8.58	0.05	0.36
6	24	7.15	0.06	0.30
7	24	5.31	0.03	0.22
8	336	41.45	0.27	0.12
9	672	40.83	0.04	0.06
10	1032	26.30	0.20	0.03

Table 30. Results of Cs concentration for sample NP-Z-0,5 3 from sample group NP-Z + KCl with the addition of ionization buffer KCl.

Number of extraction	Duration of extraction [h]	Concentration [mg·L^{-1}]	ASD	Concentration divided by extraction length [mg·L^{-1}·h^{-1}]
1	2	6.09	0.02	3.05
2	5	4.60	0.03	0.92
3	17	6.21	0.01	0.37
4	24	5.52	0.02	0.23
5	24	4.08	0.02	0.17
6	24	3.29	0.03	0.14
7	24	2.50	0.00	0.10
8	336	25.28	0.23	0.08
9	672	18.37	0.25	0.03
10	1032	13.58	0.08	0.01

Table 31. Results of Cs concentration for sample NP-Z-0,5 1 from sample group NP-Z + KCl with the addition of ionization buffer KCl.

Number of extraction	Duration of extraction [h]	Concentration [mg·L^{-1}]	ASD	Concentration divided by extraction length [mg·L^{-1}·h^{-1}]
1	2	6.61	0.06	3.31
2	5	4.56	0.01	0.91
3	17	6.39	0.03	0.38
4	24	5.73	0.01	0.24
5	24	4.05	0.01	0.17
6	24	3.46	0.05	0.14
7	24	2.52	0.01	0.11
8	336	25.59	0.17	0.08
9	672	17.42	0.11	0.03
10	1032	11.49	0.21	0.01

Table 32. Results of Cs concentration for sample NP-Z-0,5 2 from sample group NP-Z + KCl with the addition of ionization buffer KCl.

Number of extraction	Duration of extraction [h]	Concentration [mg·L^{-1}]	ASD	Concentration divided by extraction length [mg·L^{-1}·h^{-1}]
1	2	6.73	0.04	3.37
2	5	4.39	0.02	0.88
3	17	6.13	0.05	0.36
4	24	5.18	0.03	0.22
5	24	3.92	0.02	0.16
6	24	3.12	0.02	0.13
7	24	2.53	0.03	0.11
8	336	23.05	0.13	0.07
9	672	19.49	0.14	0.03
10	1032	13.27	0.06	0.01

Table 33. Results of Cs concentration for sample NM-0,5 2 from sample group NM + KCl with the addition of ionization buffer KCl.

Number of extraction	Duration of extraction [h]	Concentration [$mg \cdot L^{-1}$]	ASD	Concentration divided by extraction length [$mg \cdot L^{-1} \cdot h^{-1}$]
1	2	1.75	0.03	0.88
2	5	1.55	0.02	0.31
3	17	1.75	0.01	0.10
4	24	1.67	0.01	0.07
5	24	1.12	0.02	0.05
6	24	1.08	0.01	0.05
7	24	0.75	0.01	0.03
8	336	4.30	0.02	0.01
9	672	4.71	0.10	0.01
10	1032	3.80	0.02	0.00

Table 34. Results of Cs concentration for sample NM-0,5 3 from sample group NM + KCl with the addition of ionization buffer KCl.

Number of extraction	Duration of extraction [h]	Concentration [$mg \cdot L^{-1}$]	ASD	Concentration divided by extraction length [$mg \cdot L^{-1} \cdot h^{-1}$]
1	2	1.81	0.02	0.91
2	5	1.66	0.01	0.33
3	17	1.88	0.03	0.11
4	24	1.79	0.01	0.07
5	24	1.21	0.01	0.05
6	24	1.17	0.01	0.05
7	24	0.88	0.04	0.04
8	336	4.67	0.03	0.01
9	672	3.39	0.03	0.01
10	1032	3.86	0.03	0.00